Experimental Observations on Ice Jam Shoving

D. Healy and F. Hicks
Department of Civil and Environmental Engineering
University of Alberta, Edmonton, Alberta, Canada, T6G 2G7
fehicks@civil.ualberta.ca

The advancement of knowledge in the study of river ice jam formation processes is impeded by the lack of quantitative data describing even the most fundamental ice jam characteristics (e.g., thickness, water level, and carrier discharge). A series of experimental ice jam shoving events were observed at the University of Alberta, Edmonton, Canada, for the purpose of obtaining quantitative data describing their evolution.

For each event, an initial ice accumulation was formed under a constant carrier discharge. After the resulting accumulation stabilized the carrier discharge was stepped rapidly to a higher constant value to initiate failure of the original accumulation. Two events were selected for presentation in this paper to illustrate ice jam shoving events for both a proportionally *high* (85%) and proportionally *low* (30%) increase in discharge. The techniques used to obtain continuous water level, accumulation thickness, and discharge data are presented along with an estimate on the accuracy of the data.

1.0 Introduction

The progression of knowledge encompassing the phenomena of ice jam shoving has been impeded by a lack of quantitative ice jam data. Both logistical and safety related reasons have made obtaining quantitative data in the field nearly impossible. A safe and practical alternative to obtaining field data is to conduct experimental investigations under controlled laboratory conditions.

The work presented in this paper represents a small portion of a larger ongoing experimental ice jam investigation underway at the University of Alberta, Edmonton, Alberta, Canada. The results of two experimental ice jam shoving events were selected to represent different failure progressions. Failures (shoving) for both experimental events were initiated by a rapid increase

in carrier discharge. The relative increases in carrier discharge were approximately 30% for the first event and 85% for the second.

Experimental studies to date have been limited either to steady flow (Saade and Sarraf, 1996) or to more qualitative observations on unsteady processes (Zufelt, 1990, 1992). The preliminary results presented herein represent the first quantitative observations on ice jam shoving initiated by a rapid increase in discharge and may provide insight for researchers and practitioners concerned with the affects of rapid increases in discharge on stable ice accumulations. Ultimately, experimental data obtained during the more comprehensive study will be made available for the purpose of increasing the understanding of dynamic ice jam processes. An ancillary benefit to this research will be the availability of quantitative data for researchers whom have developed or are developing dynamic ice jam process models.

The intent of this paper is simply to share some of these early observations on experimental ice jam shoving with interested researchers. Detailed interpretation of the data obtained from these ongoing experiments will follow at the completion of the entire study.

2.0 Experimental Apparatus and Procedures

Figure 1 presents a schematic of the experimental setup used in this study which was similar to that used in preliminary investigations (Hicks and Healy, 1999) carried out in a 30.5 m long recirculating flume located in the T. Blench Hydraulics Lab at the University of Alberta. This rectangular flume (see figure 2) has 0.91 m high side walls and a width of 1.22 m. The bed is sheet metal (though slightly rusted and rough in texture) and the walls are plexiglass. Modifications to the original setup included: a new supply pump for carrier discharge; a continuous water level recorder at the flume outlet; and the addition of a coarse wire mesh along the flume sidewalls. A unique relationship between discharge and depth was found over the weir located at the downstream end of the flume (station 30 m). The placement of a continuous water level recorder at this location facilitated a reliable estimate of carrier discharge exiting the system (i.e. the downstream boundary condition). The wire mesh was attached to the sides of the flume in an attempt to better model ice interaction at the banks. During shoving events, an “ice-ice” shear interface was observed along the edge of the flume walls. This “ice-ice” interface was believed to better represent natural conditions. The wire mesh that was attached to the side of the flume can be seen in the background of Figure 3 which illustrates the surface texture or roughness of a typical accumulation after shoving.

Discharges up to 65 L/s were supplied to a head tank via a 0.20 m diameter pipe. Flow straigheners in the floor of the head box condition the flume's inflow. At the downstream end of the flume, water levels are controlled with a 0.15 m high rounded weir as well as with a series of adjustable vertical vanes spaced across the channel. The flume was kept constant to its maximum attainable slope of 0.00164.

Ice floes were simulated using polyethylene pieces with a specific gravity of 0.92. A mixture of sizes were used ranging from 1.27 x 1.27 x 0.32 up to 5 x 5 x 0.6 cm. The mixture had a bulk porosity of 0.49, and a dry angle of repose of 37°.

A 1.9 mm x 1.22 m x 1.22 m sheet of plywood was positioned 24.5 m downstream of the head box to simulate an intact ice cover in the downstream portion of the flume. Rigid insulation extended downstream of the plywood an additional 4.8 m towards the end of the flume. Both the sheet of plywood and rigid insulation were allowed to float freely. A wire mesh was fastened to the upstream edge of the plywood to facilitate the control of the thickness and location of the toe of the jam. At the beginning of each experiment a steady discharge was introduced under open water conditions with the plywood sheet and rigid insulation in place. The flow was allowed to stabilize and then a water surface profile was measured.

The model ice was fed into the flow manually with the aid of a hopper located at the upstream end of the flume (see figure 4). A piece of rigid plastic was used as a chute to guide the pieces into the flow with a minimum of disturbance. The total time required to deliver the ice pieces to the flume was approximately 14 minutes for both tests presented herein. Once all of the ice was in, the location of the head of the accumulation was monitored, as was the leading edge of the ice while the ice cover developed. Variations in flow depth and ice thickness were monitored with video cameras at stations 10 and 20 m downstream of the head tank. Once the ice cover had stabilized and reached near steady state conditions (after about 1 hour) water surface and ice thickness profiles were measured. The bottom ice profile was measured approximately by estimating the average thickness across the jam for each measurement section from the side of the flume.

Flow rates in the supply line were measured with a magnetic flow meter, and flow velocities were measured during ice jam formation using Prandtl tubes and pressure transducers. All discharge and velocity measurements were captured digitally using a Pentium computer running the LabView© data collection software program. The Prandtl tubes were positioned on the flume centreline at stations 10 and 20 m downstream of the head tank. The Prandlt tubes were positioned so as to try and best capture the 20% and 80% depths before and after the model jam shoved, to obtain an estimate of the mean velocity on the channel centerline which was then related to the total section average velocity.

3.0 Data Collection

Figure 1 presents a schematic of the locations where continuous data was recorded for each event. The following parameters were measured (sample rate = 1 Hz) directly and recorded to a digital file using a PC and the LabView© data collection software program: carrier discharge (measured from the magnetic flow meter); velocities at stations 10 and 20 m (measured using Prandlt tubes and pressure transducers); and the depth of flow over the weir at the downstream end (using a capacitance model water level transmitter). The date and time associated with each sample was attached to the digital file. In addition to the digitally recorded data, water level and ice thickness data were recorded visually at stations 10 and 20 m using video cameras; these images were processed through a multiplexer to facilitate recording on a single VHS tape. A date and time stamp was added to the images by the multiplexer to enable synchronization of the video data with the digitally recorded data.

After the discharge was increased and the onset of shoving began, the progression of the initial accumulation was tracked manually by persons or "particle trackers" who followed "tracking particles" placed on the surface of the initial accumulation prior to the rapid increase in discharge (see Figure 5). Ultimately, when near steady state conditions were observed (i.e. when the ice cover appeared to have stabilized with no further perceptible movement of the ice pieces) "static" water surface and ice thickness profiles were recorded using a point gauge.

4.0 Estimation of Discharge at Stations 10 and 20 m

Discharge was estimated through interpretation of continuous velocity data, water surface elevation, and submerged ice thickness. Three Prandlt tubes were positioned on the channel centerline at 20% and 80% of the estimated average of the initial and final flow depths at measurement stations 10 and 20 m. Depth of flow at stations 10 and 20 m were deduced from continuous water level and ice thickness data recorded on video. Point velocities taken at the measurement stations were used to estimate average velocity at the channel centerline. Steady flow calibration runs were conducted to determine the relationships between the mean centreline velocity and the mean velocity in the channel at both of these stations for both open water and ice covered conditions. These relationships were obtained by relating the mean velocity for profiles measured along the channel centerline to the average channel velocity based on the measured steady discharge. This average velocity for the entire cross section, together with the varying water level and ice thickness documented with the video camera, facilitated the calculation of the discharge at stations 10 and 20 m.

5.0 Formation of an Initial Accumulation

The initial accumulations for both tests were formed under a constant carrier discharge of approximately 34 L/s. Figure 6 illustrates the general processes observed during the formation of the initial cover. During formation, ice accumulated through a combination of juxtaposition, underturning, and hydraulic transport. As the model ice is first arrested (at either the floating toe or progressing head of the accumulation) it tended to juxtapose, with pieces rearranging themselves to provide a complete cover of ice over the open water approximately one layer thick. In conjunction with the process of juxtaposition, some of the ice pieces wound underturn and deposit directly under the piece immediately downstream without becoming entrained in the flow (figure 6 (a)&(b)). Other pieces would be become entrained in the flow and were transported hydraulically where they deposited downstream of the progressing head. This active portion of the accumulation where the model ice was transported and deposited downstream of the leading edge of the accumulation extended approximately one to one and a half channel widths downstream from the leading edge (figure 6 (c)&(d)).

6.0 Failure of an Initial Accumulation (Shoving) due to a Rapid Increase in Discharge

6.1 Mobilization and Progression of the Initial Accumulation

After the initial accumulation had stabilized the discharge was stepped rapidly by manually opening a valve on the supply line. Figure 7 illustrates: the discharge values recorded by the

magnetic flow meter (carrier discharge); the discharge at station 30 m (downstream boundary); and water levels at stations 10 and 20 m. After the discharge was increased it remained constant. The time to peak for the carrier discharge was 5 seconds for the first test (30% increase in discharge) and 13 seconds for the second test (85% increase in discharge). This form of rapid increase was implemented to ensure a dynamic (surge) event. The travel time for the stepped wave to pass through the system was approximately 20 seconds for both tests.

Shortly after the stepped increase in discharge the water surface rose at measurement stations 10 and 20 m. Figure 7 illustrates the variation in water levels at stations 10 and 20 m (for both tests) and indicates the time of the first observed movement of the cover (mobilization).

As the ice cover thickened little to no underturning or under ice transport was observed; this implies that the cover failed mostly in a telescopic manner by shoving. The progression of the ice cover was recorded by tracking particles placed on the surface of the accumulation (prior to mobilization) near stations 10, 15, and 20 m downstream from the head tank. The progression of the tracking particles at these three locations along with the progression of the upstream limit or "head" of the accumulation were recorded manually. Figure 8 illustrates the rate of progression for the surface of the cover for both tests (30% and 85% increase in discharge). For both tests, the ice in the upstream portions of the accumulation moved a greater distance than ice in the downstream portions. Also, the rate of ice cover progression decreased asymptotically to its final static position. It is interesting to note that for the test with the proportionally low increase in discharge (30%), the cover appeared to stabilize momentarily after approximately 6 minutes and then experienced another period of movement before reaching the final stable condition, while the higher discharge consolidated at a more continuous rate.

6.2 Initial and Final Static Accumulations

Figure 9 illustrates the observed water surface and bottom of ice profiles for the initial and final stable accumulations. Based on the measured initial and final stable ice accumulations, the volume of water that went into storage was 0.46 m^3 for test 1 and 1.64 m^3 for test 2. Table 1 provides a summary of some of the salient geometric features of these accumulations.

Table 1. Salient geometric features of initial and final stable accumulations.

	30% Increase in Discharge		**85% Increase in Discharge**	
	Initial	**Final**	**Initial**	**Final**
Discharge (L/s)	35	44	35	62
Length (m)	19.5	14.7	18.5	6.3
Submerged bulk volume (m^3)	0.61	0.64	0.52	0.58
Total bulk volume (m^3)	0.66	0.70	0.56	0.63
Average thickness (cm)	2.8	4.0	2.5	7.8
Porosity	0.48	0.51	0.39	0.46

The submerged volume was determined by integrating the measured thickness values over the length of the stabilized accumulations. The total bulk volume was calculated by dividing the submerged bulk volume by the specific gravity of the model ice material (0.92). The average thickness of the accumulation represents the total bulk volume divided by the product of the measured length of the accumulation and width of the flume (1.2 m). The volume of ice added to both tests was 0.34 m^3, which represents the total volume of the actual model ice material (i.e. not the bulk volume). The porosity of the accumulation is simply the ratio between the volume of voids to the total bulk volume of ice in the accumulation. The porosity was assumed to be equivalent both above and below the water surface.

Measurements of ice thickness were based on visual interpretation of the average thickness across a given section and were recorded to the nearest 0.5 cm. It is possible that errors of up to 0.25 cm were involved in the thickness measurements. For a 20 m length of accumulation errors in the thickness measurement would translate to a maximum error in volume calculations of 0.06 m^3 (approximately 10% of the values shown in Table 6.1).

6.3 Variation in Water Level, Thickness, and Discharge during Cover Progression

Figures 10 through 13 present the measured variation in the following parameters: centerline point velocities recorded using Prandlt tubes and pressure transducers at stations 10 and 20 m; water surface and ice thickness at stations 10 and 20 m; carrier discharge; estimated discharge at stations 10 and 20 m; and discharge at station 30 m (downstream boundary).

Prandlt tubes or "probes" were placed in pairs at both measurement stations 10 and 20 m to record continuous centerline velocities (box (a), figures 10 – 13). Probe locations 1 and 2 were placed so as to try and capture centerline point velocities at 20% and 80% of the depth, respectively. During both tests, the probes remained fixed as the ice thickness and water levels varied. Consequently, the 20% and 80% depths of flow deviated from the probe locations (box (b), figures 10 – 13). Table 2 summarizes the maximum observed deviation of the 20% and 80% flow depths from the probe locations.

Table 2. Maximum deviation of 20% and 80% depth of flow from fixed probe locations as a percentage of the total depth of flow.

	Station 10 m	**Station 20 m**
Test 1		
Probe location 1	-9%	+8%
Probe location 2	-3%	+2%
Test 2		
Probe location 1	+27%	-15%
Probe location 2	-15%	+7%

Box (c) in figures 10 – 13 presents the estimated continuous discharge values for measurement stations 10 and 20 m. For mass to be conserved, the volume of water that goes into storage should be equivalent to the integrated difference between the carrier discharge and the discharge at station 30 m, the downstream boundary (inflow – outflow). Table 3 summarizes the storage volumes calculated in this manner and compares these values to the storage volume estimates based on the initial and final ice accumulation profiles (calculated previously).

Table 3. Storage volume estimates.

	Test 1 (Q ↑ 30%)	**Test 2 (Q ↑ 85%)**
Storage volume based on inflow – outflow.	0.49 m^3	1.59 m^3
Storage volume based on initial and final ice accumulation profiles.	0.46 m^3	1.64 m^3
Difference between calculated storage volumes.	6%	3%

The discharge estimates at stations 10 and 20 m were not equivalent to the carrier discharge prior to the rapid increase in discharge or after the rapid increase when flow conditions reached a steady state. Under steady state conditions the discharge at stations 10 and 20 m would be expected to be equivalent to the carrier discharge. The percent variation in discharge at stations 10 and 20 m from the carrier discharge were calculated in an attempt to try and quantify errors associated with these estimates. Figure 14 presents this variation for both tests where the variation in discharge from the carrier discharge is approximately 10%. Therefore, as a first estimate, the estimated discharges at station 10 and 20 m can be considered accurate to within 10%.

7.0 Discussion

The results of the two test presented herein are representative of a group of approximately two dozen tests that have already been conducted at the University of Alberta. The other tests span a range of relative rapid increases in discharge and initial flow conditions. The reduction and initial analyses of these other tests is underway; consequently, no attempt has been made to analyze the results of all tests as a whole. Based on the experience gained during this first series of tests, slight modifications to the testing procedures will be introduced for the next series of tests. For example, the probes will be introduced from the beneath the floating ice accumulation to limit any interference of the probes on ice accumulations. Also, a series of video cameras will be positioned directly above the flume to aid in the tracking of the cover progression. Plans are also underway for the investigation of an ice jam forming from the result of an “ice run” arresting at a solid cover.

8.0 References

Healy, D. and Hicks, F. 1999. An Assessment of the Applicability of Steady Flow Ice Jam Profile Models. Proceedings of the 10th Workshop on the Hydraulics of Ice Covered Rivers, Winnipeg, June 1999, pp. 185-195.

Saade, Raafat G. Sarraf, S. 1996. Phreatic water surface profiles along ice jams – an experimental study. Nordic Hydrology; 27(3): 185-201.

Zufelt, J.E. 1990. Experimental observations of shoving and thickening: Comparison to equilibrium thickness theory. IAHR Proceedings of the International Symposium on Ice, 10th, Espoo, Finland, 1990, v.1: 500-510.

Zufelt, J.E. 1992. Modes of ice cover failure during shoving and thickening. IAHR Proceedings of the International Symposium on Ice, 11th, Banff, Alberata, Canada, v.3: 1507-1514.

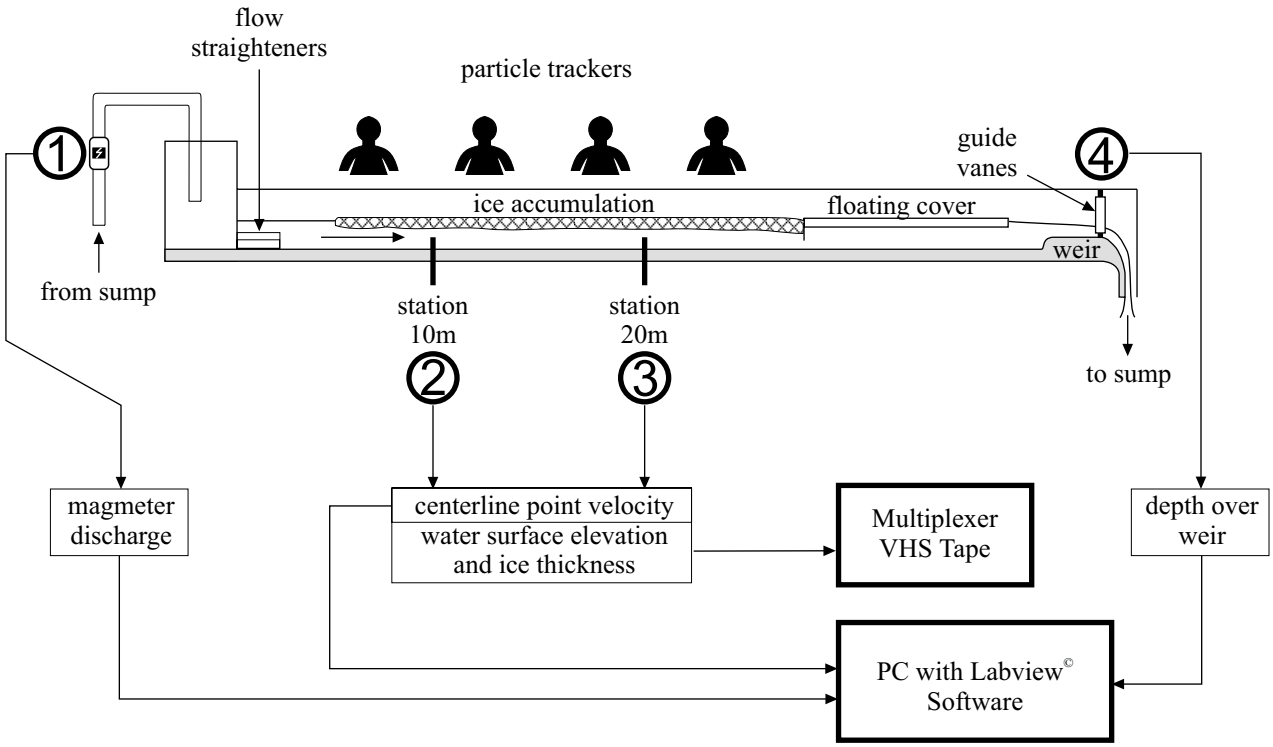

Figure 1. Experimental setup and data collection schematic.

Figure 2. Experimental flume - looking upstream,
T. Blench Hydraulics Laboratory, University of Alberta.

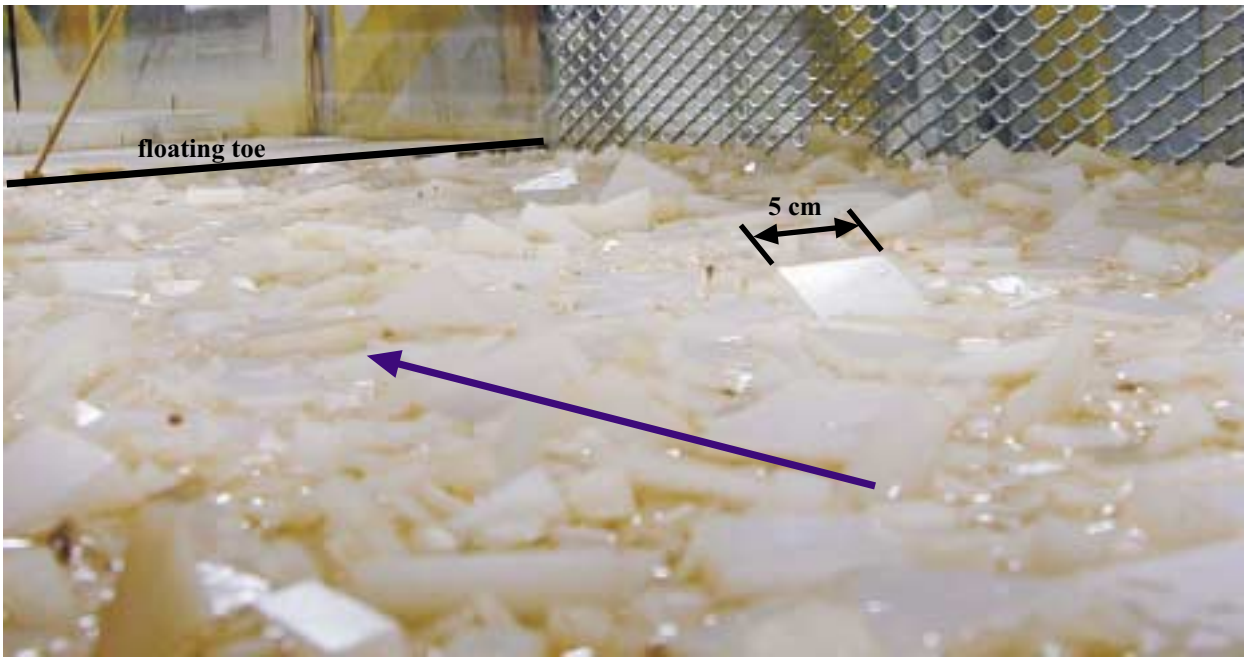

Figure 3. Surface texture (roughness) of ice cover after shoving event.

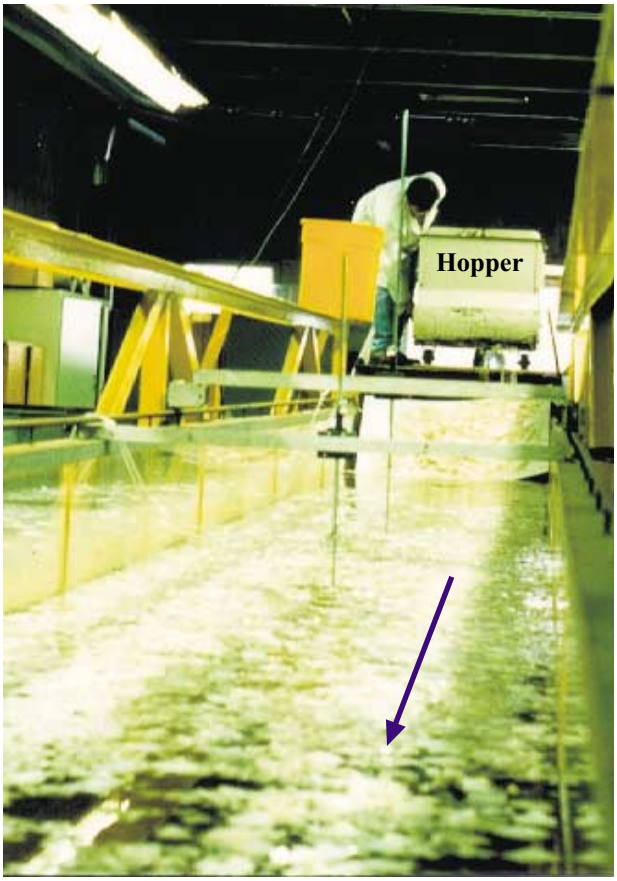

Figure 4. Loading ice for initial accumulation.

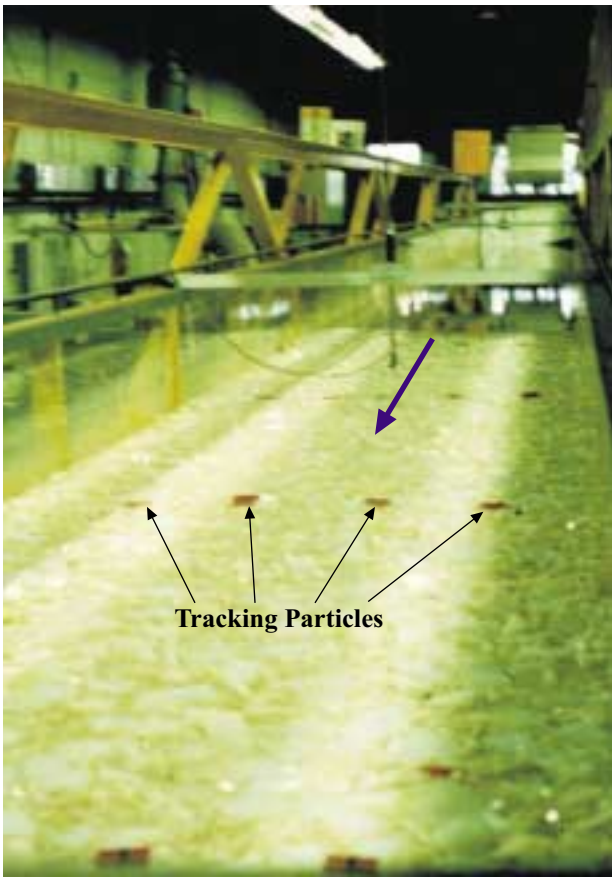

Figure 5. Placement of tracking particles on surface of initial accumulation.

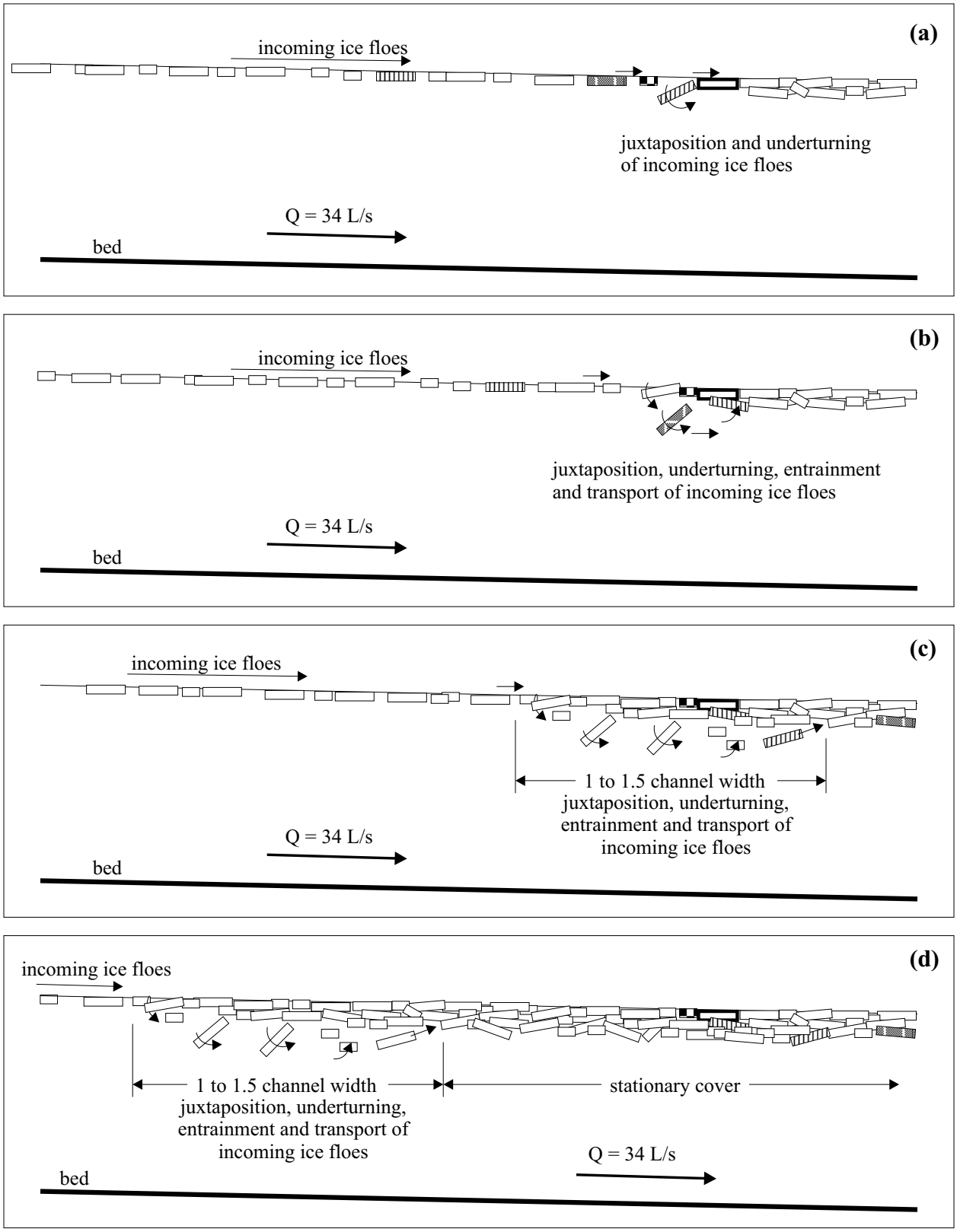

Figure 6. Development of initial ice accumulation.

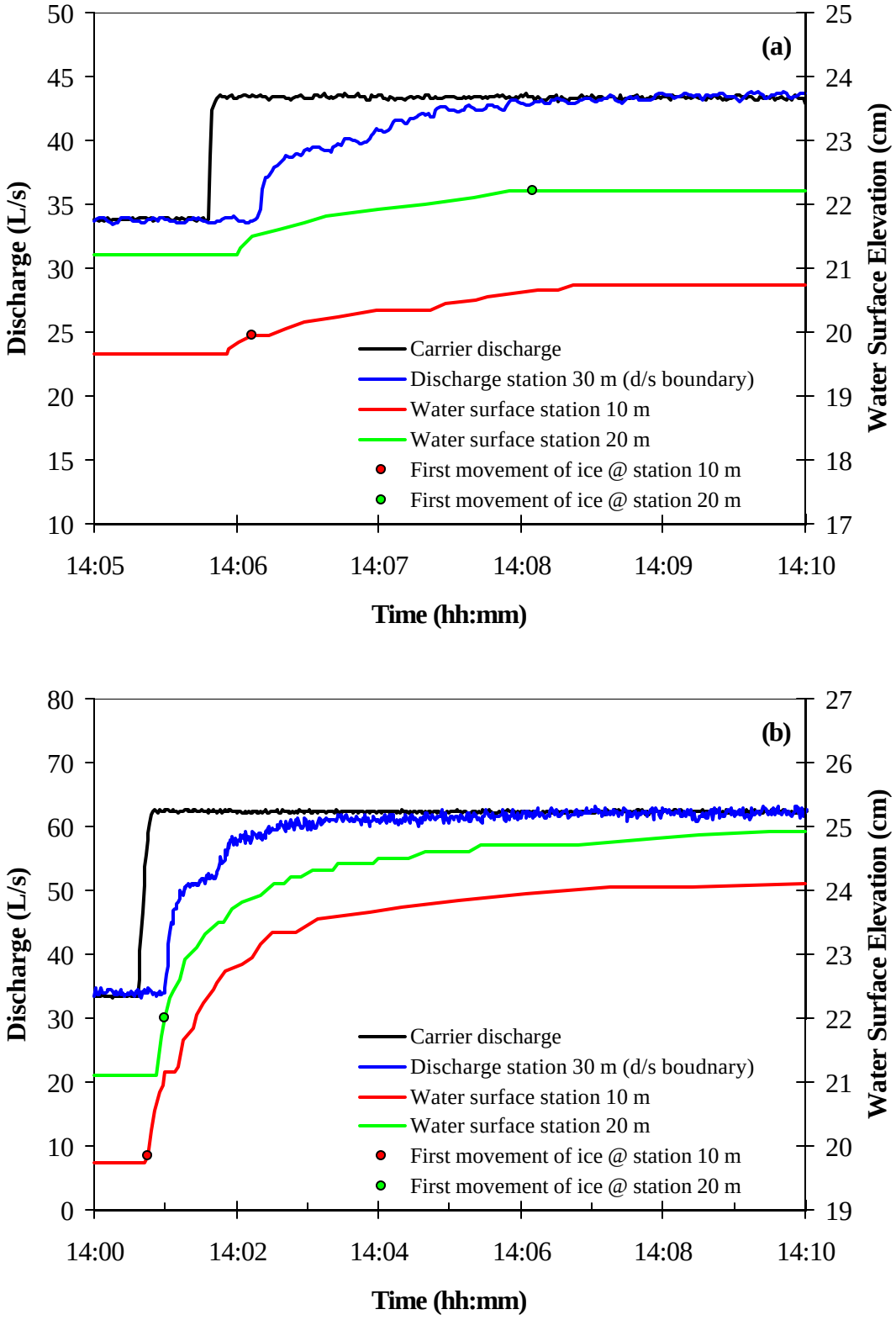

Figure 7. Continuous discharges and observed water levels during shoving of ice accumulation for (a) 30% increase in discharge and (b) 85% increase in discharge.

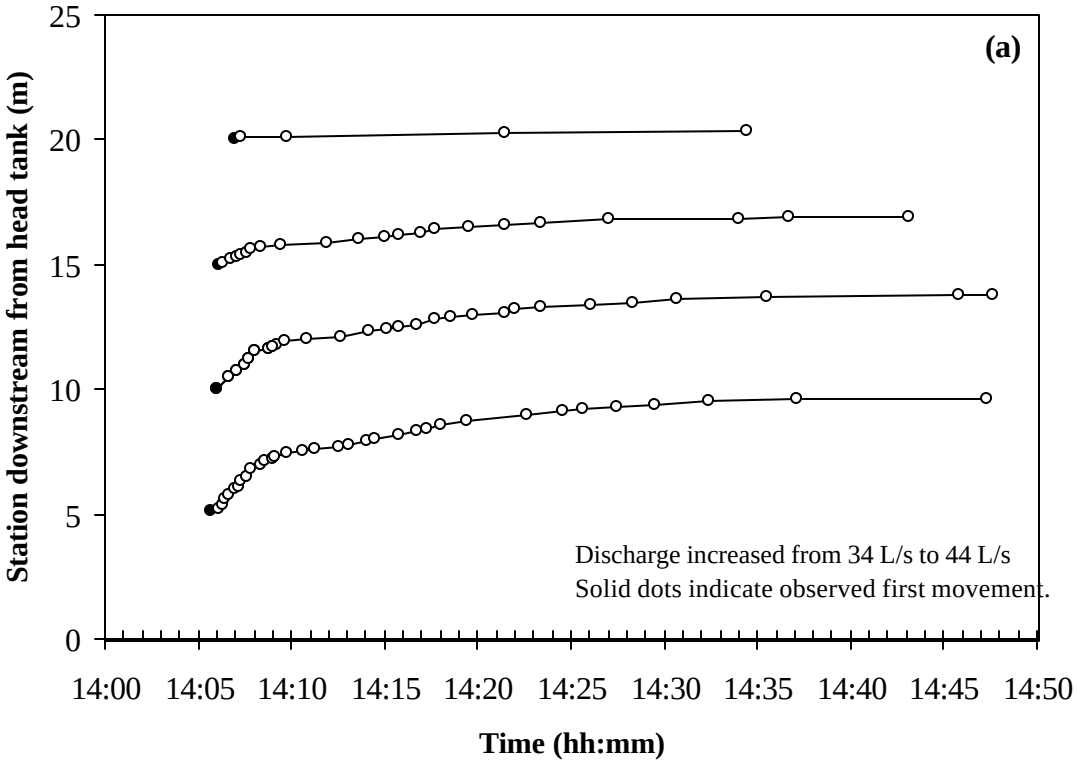

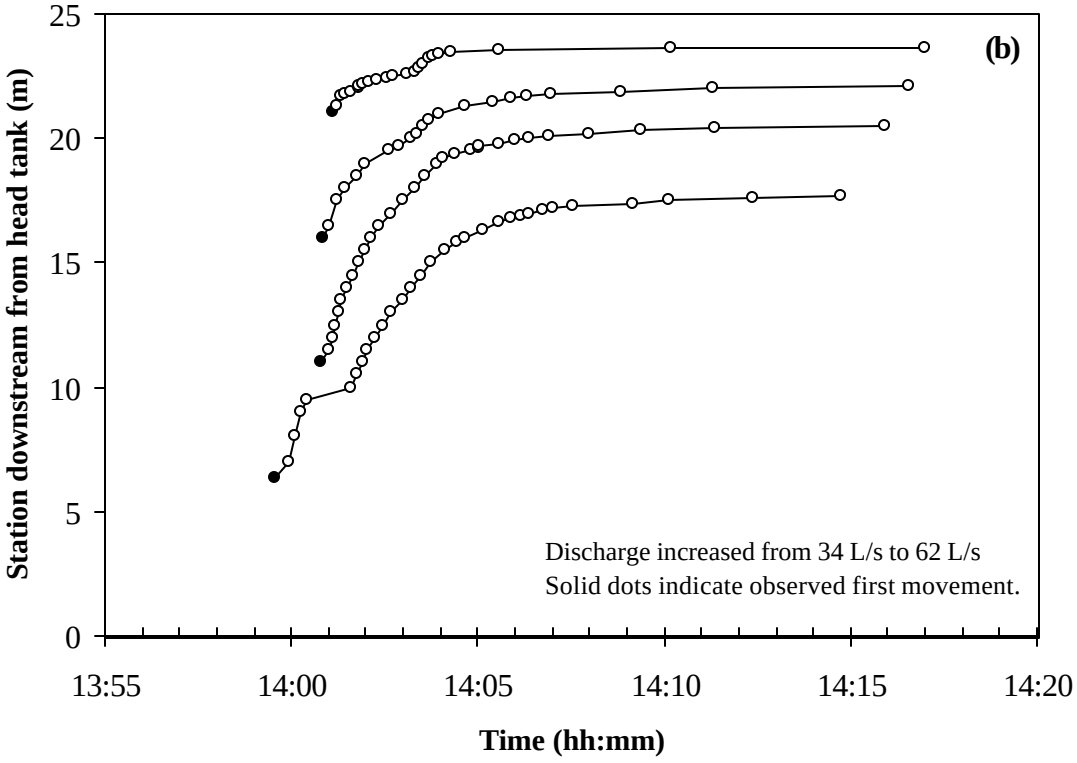

Figure 8. Propagation of tracking particles placed on the surface of the initial accumulation following (a) 30% increase and (b) 85% increase in discharge.

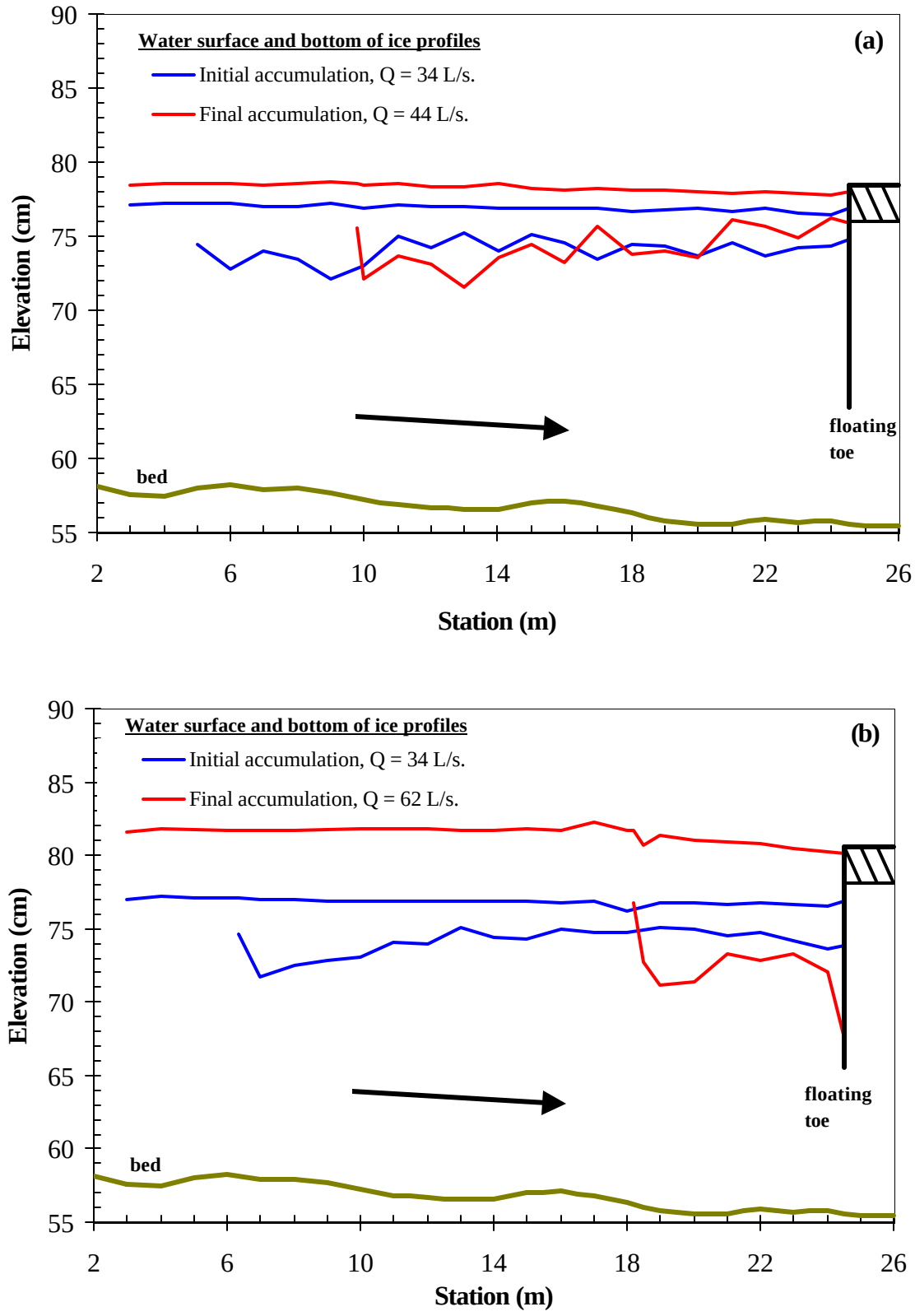

Figure 9. Water surface and bottom of ice profiles for initial and final accumulations for (a) 30% increase in discharge and (b) 85% increase in discharge.

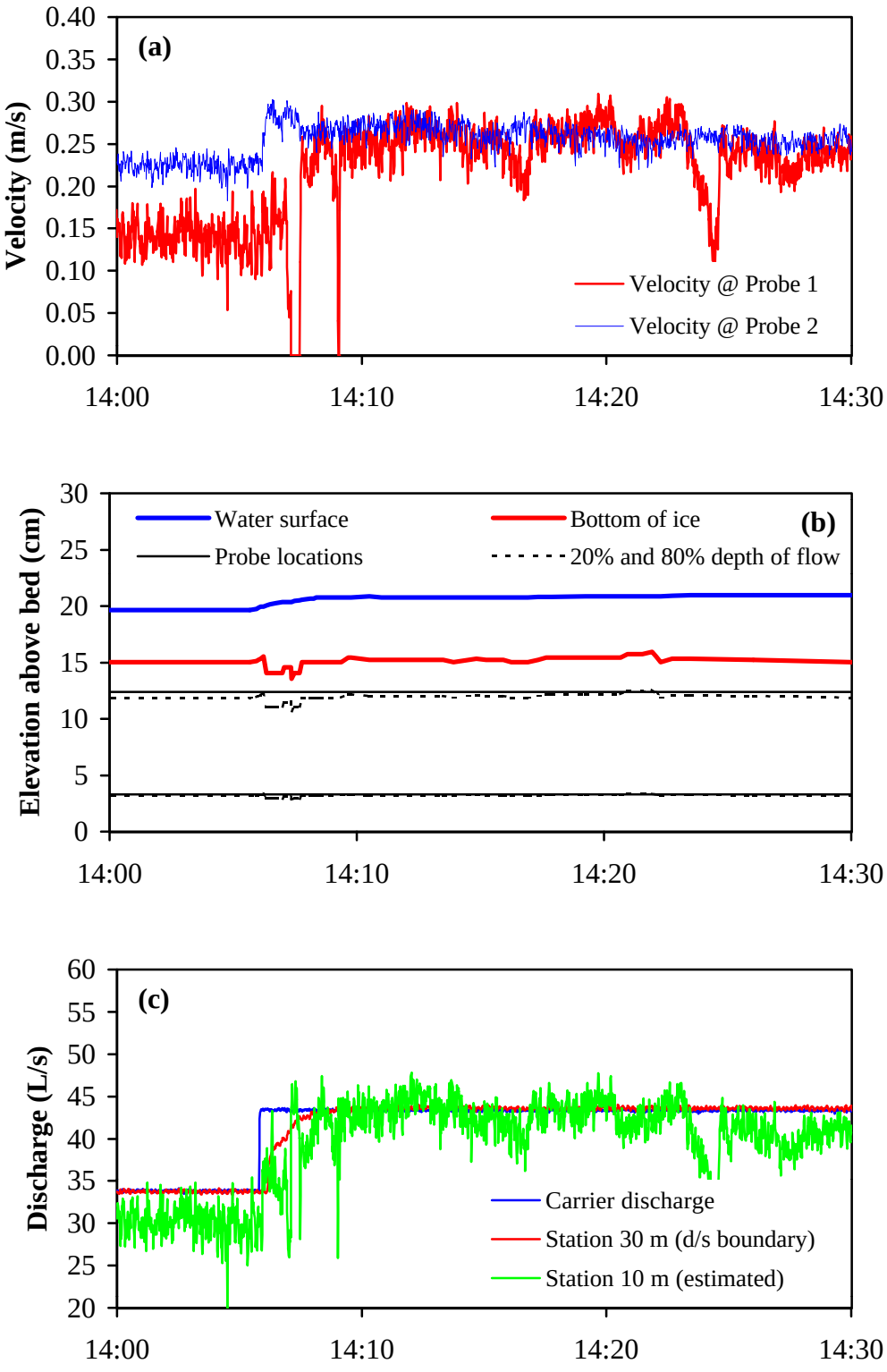

Figure 10. Test 1 - Continuous velocity, depth, ice thickness, and estimated discharge at station 10m.

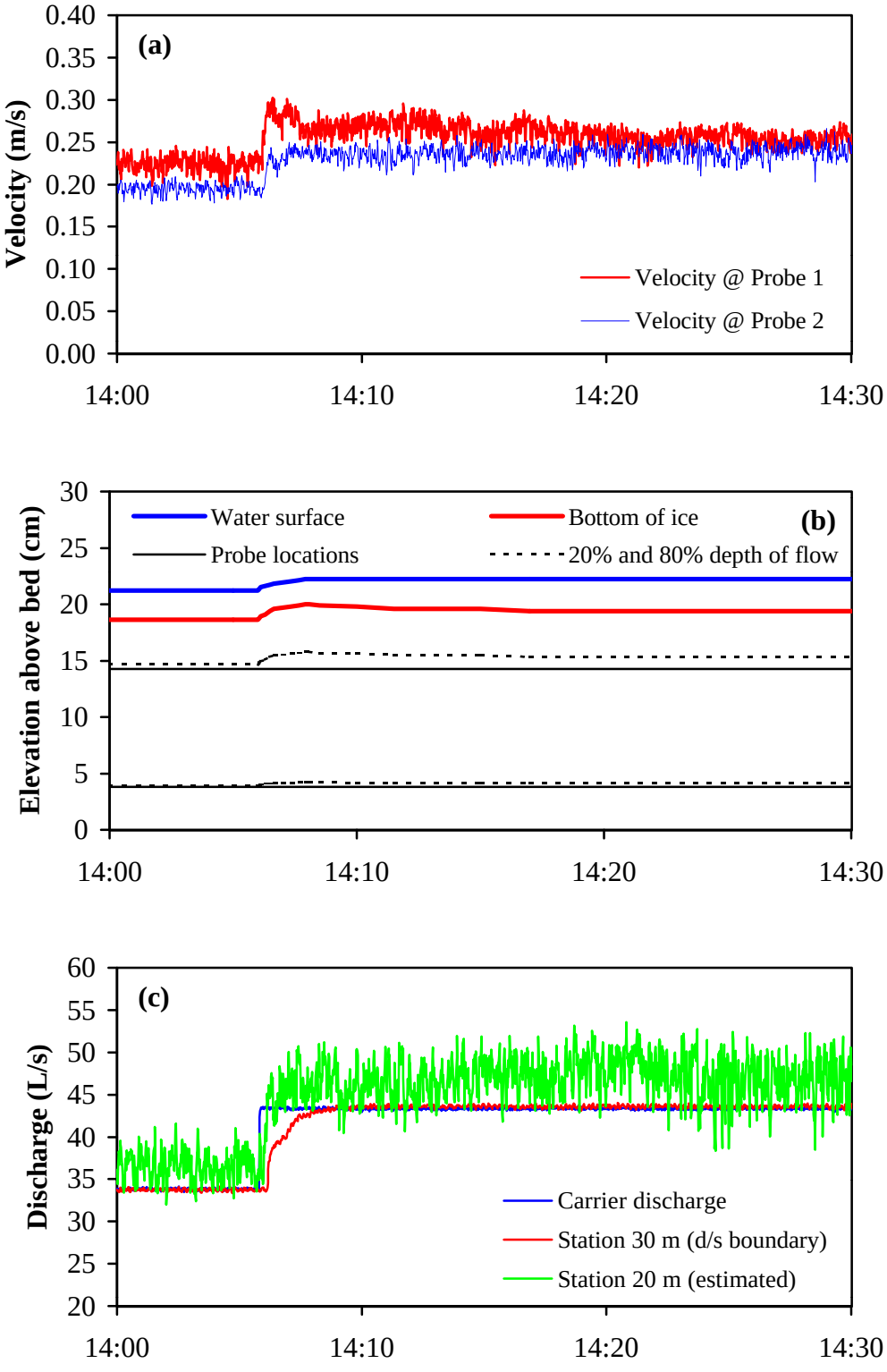

Figure 11. Test 1 - Continuous velocity, depth, ice thickness, and estimated discharge at station 20m.

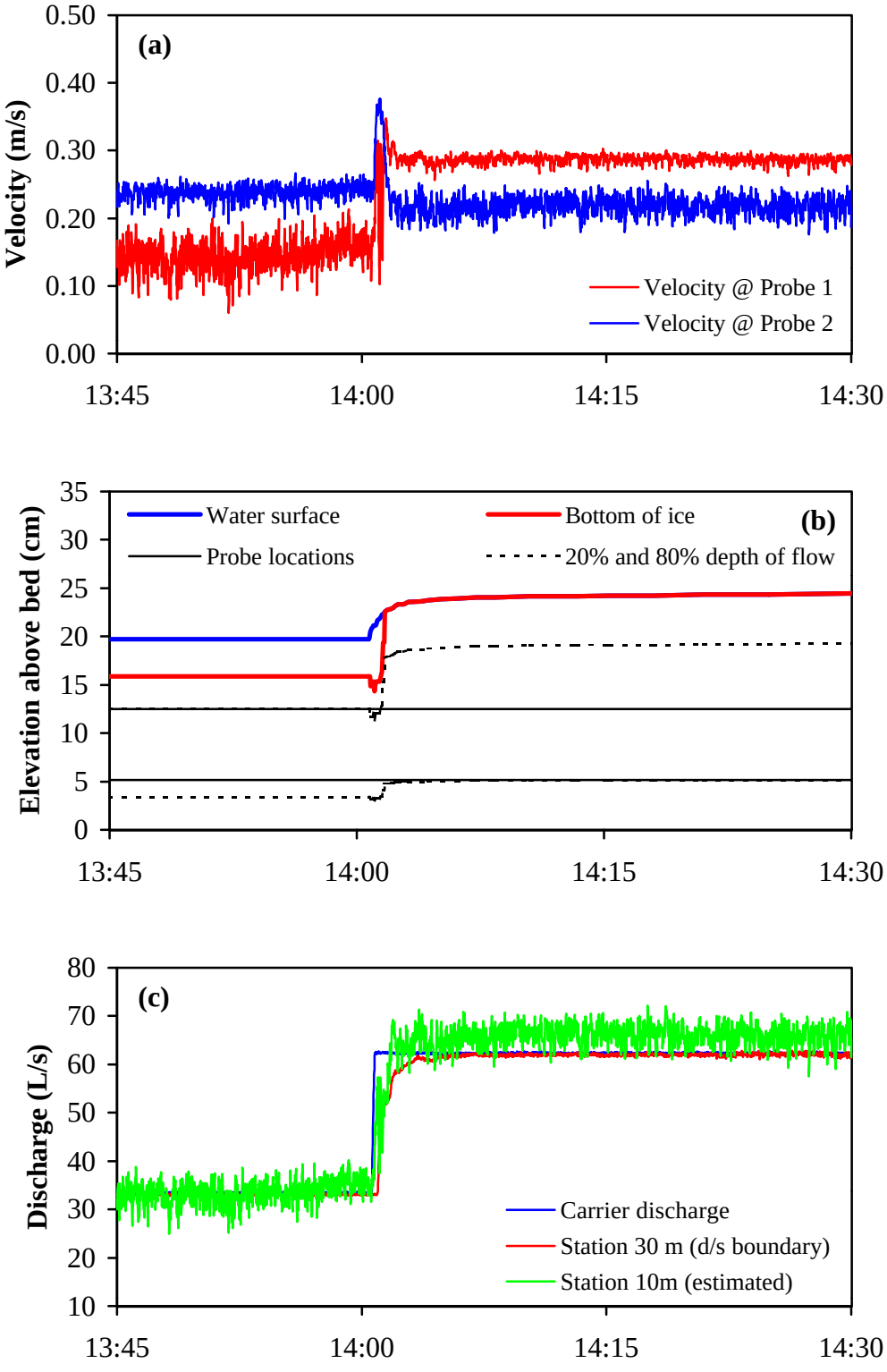

Figure 12. Test 2 - Continuous velocity, depth, ice thickness, and estimated discharge at station 10m.

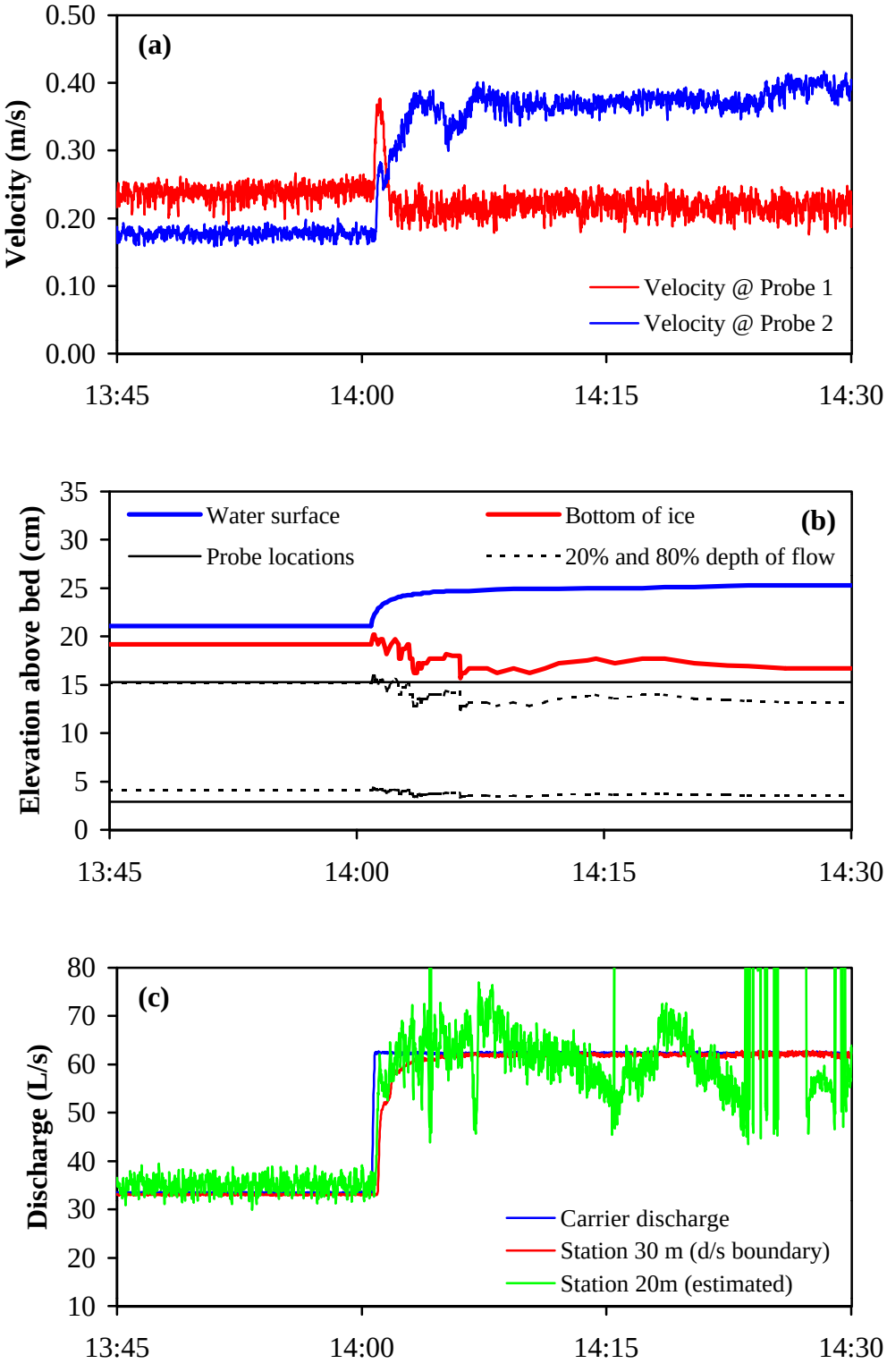

Figure 13. Test 2 - Continuous velocity, depth, ice thickness, and estimated discharge at station 20m.

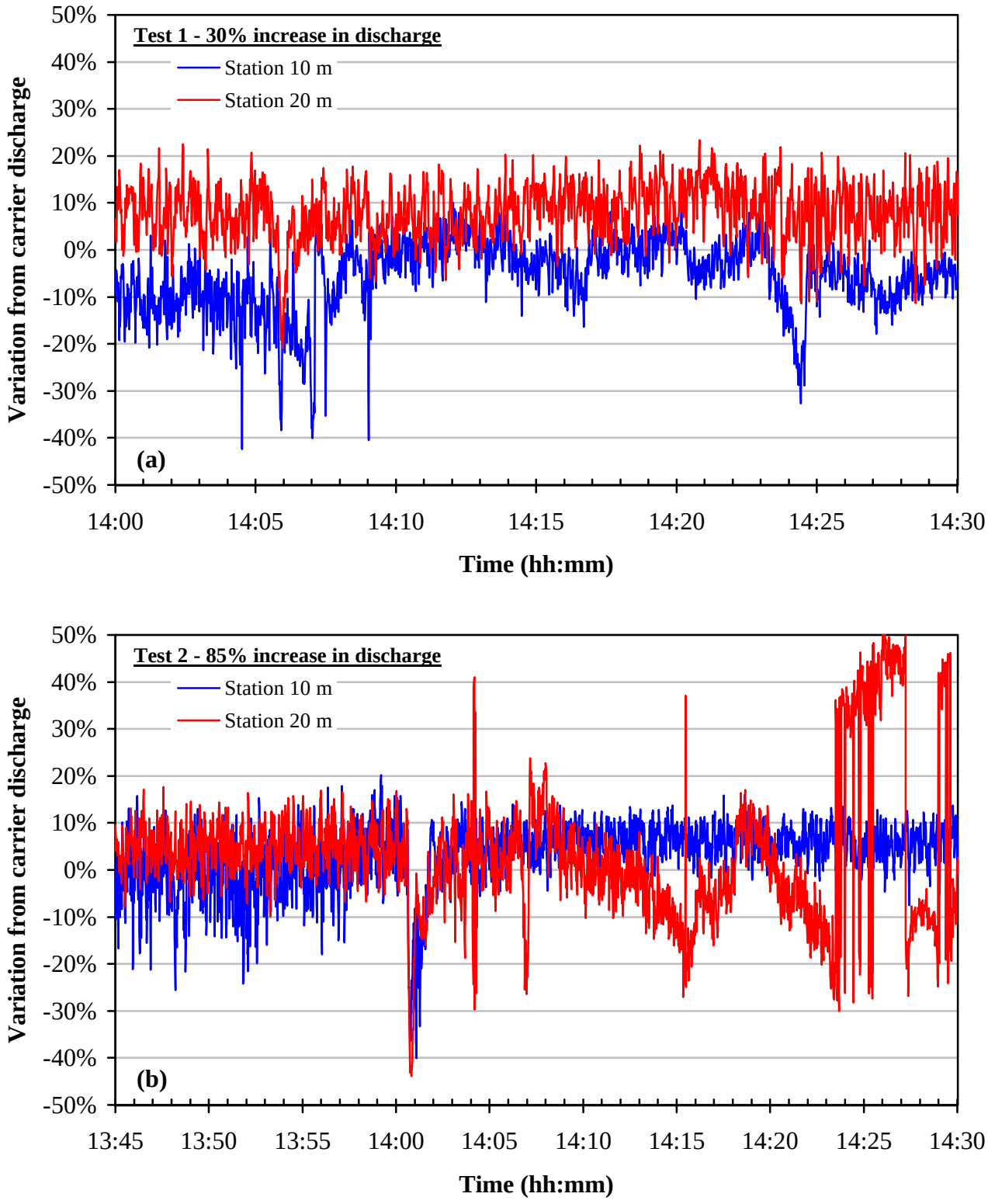

Figure 14. Variation of estimated discharge at stations 10 and 20 m from carrier discharge for (a) 30% increase in discharge and (b) 85% increase in discharge.